Statistica Sinica Preprint No: SS-2018-0214	
Title	Testing First-Order Spherical Symmetry of Spatial Point Processes
Manuscript ID	SS-2018-0214
URL	http://www.stat.sinica.edu.tw/statistica/
DOI	10.5705/ss.202018.0214
Complete List of Authors	Tonglin Zhang and Jorge Mateu
Corresponding Author	Tonglin Zhang
E-mail	tlzhang@purdue.edu
Notice: Accepted version subject to English editing.	

Testing First-Order Spherical Symmetry of Spatial Point Processes

Tonglin Zhang and Jorge Mateu

Purdue University and Universitat Jaume I

Abstract: This article proposes a Kolmogorov-Smirnov-type test to assess spherical symmetry of the first-order intensity function of a spatial point process (SPP). Spherical symmetry, which is an important assumption in the well-known ETAS (epidemic type aftershock sequence) model, means that the intensity function of an SPP is invariant under a spherical transformation in an Euclidean space. An important property of first-order spherical symmetry is that the expected number of points within a sector region is proportional to the angle measure of the region. This provides a way to construct our test statistic. The asymptotic distribution of the test statistic is obtained under the framework of increasing domain asymptotics with weak dependence. We show that the resulting test statistic converges weakly to the absolute maximum of a zero mean Gaussian process under the null hypothesis and it is also consistent under the alternative hypothesis. A simulation study shows that the type I error probability of the test is close to the significance level, and the power increases to one as the magnitude of non-spherical symmetry increases. In an application of the ETAS model to Japan earthquakes, the article concludes that the first-order spherical symmetry assumption can be roughly accepted.

Key words and phrases: Gaussian processes; Intensity functions; Kolmogorov-Smirnov test; Polar transformation; Spatial point processes (SPPs); Spherical sym-

metry.

1. Introduction

Spatial point processes (SPPs) are widely applied in a variety of scientific disciplines such as forestry (Stoyan, 1994), epidemiology (Diggle, 2006), wildfires (Peng, Schoenberg, and Woods, 2005), and earthquakes (Ogata, 1988). In the literature, an SPP is treated as a pattern of points for locations of random events developed in a complete separable metric space or a bounded subset of the space. Point distributions and dependence structures are modeled by intensity functions (Diggle, 2003). The simplifying assumptions of stationarity and isotropy have been developed to make the analysis of SPPs convenient. Various well-known tools have been proposed. Examples include the K-function (Ripley, 1976), the L-function (Besag, 1977), and the pair correlation function (Stoyan and Stoyan, 1996). Because of its importance, a few methods have been proposed to assess stationarity (Guan, 2008; Zhang and Zhou, 2014). A recent interest is to model SPPs under nonstationarity (Møller and Waagepetersen, 2007). An important concept called the second-order intensity-reweighted stationarity (SOIRS) has been proposed (Baddeley, Møller, and Waagepetersen, 2000). The concept is powerful in the joint analysis of the first-order and second-order intensity functions under nonstationarity. With the aid of SOIRS, a number of methods for nonstationary SPPs have been proposed (Guan and Shen, 2010; Henrys and Brown, 2009; Waagepetersen, 2007).

SOIRS only provides the relationship between the first-order and the second-order intensity functions. It does not specify any assumptions for the first-order intensity function. Therefore, assumptions for the first-order intensity functions can be proposed independently. It provides an opportunity to develop models only for the first-order intensity function, and simultaneously address the second-order properties. Many methods have been developed. Examples include parametric and nonparametric estimation (Diggle, 1985), Bayesian estimation (Myllymäki and Penttinen, 2009), proportionality (Zhang and Zhuang, 2017), and separability (Zhang, 2014, 2017). Although they are useful in practice, an important question about whether the first-order intensity function has a spherically symmetric structure has not been studied. The purpose of this article is to propose a formal statistical test to address this problem.

Spherical symmetry is an important assumption of the well-known ETAS (epidemic type aftershock sequence) model. It is one of the earliest point process models created for clustered events. The ETAS is a parametric model defined by a conditional intensity function for mainshock and aftershock earthquakes. It is originally developed for earthquakes (Zhuang, Ogata, and Vere-Jones, 2002) and later extended to infectious diseases (Meyer and Held, 2014) and invasive species (Balderama, et. al, 2012). In the ETAS model, events in each aftershock cluster are independently produced by their corresponding mainshock earthquakes (ancestors). The size of the aftershock cluster depends on the magnitude of its ancestor. If there is only one extremely large ancestor, then within a certain

period the entire earthquake pattern is primarily dominated by the ancestor and its aftershocks. Therefore, our approach can be used to justify assumptions of the ETAS model, although our interest is far beyond.

Our approach is motivated by classical tests for spherical symmetry of multivariate distributions. Spherically symmetric distributions are natural extensions of the multivariate standard normal distribution. The spherically symmetric multivariate distribution, which can be traced back about thirty years ago (Hall, Watson, and Cabrera, 1987), is well-known in the literature. The focus is either estimation (Brandwein and Strawderman, 1991) or hypothesis testing (Henze and Meintanis, 2014) based on an identically and independently distributed sample. Because of the existence of dependence, these approaches cannot be used to assess spherical symmetry of SPPs. Therefore, new approaches are needed.

We propose a Kolmogorov-Smirnov-type statistic to assess spherical symmetry. The dependence structure is described by a scale parameter in the test statistic. The p-value is calculated by its asymptotic null distribution. We evaluate the properties of our test by simulations and applications. In simulations, we study type I error probabilities and power. We conclude that the type I error probabilities are always close to the significance level, and the power function always increases to 1 as the magnitude of non-spherical symmetry increases. For illustration, we apply our test to an earthquake data set. We conclude that spherical symmetry assumption is generally correct at the beginning of the oc-

currence of a great earthquake, indicating that the ETAS model can capture major characteristics of earthquake aftershock patterns.

To the best of our knowledge, our approach is the first formal test for spherical symmetry of SPPs. As the test statistic is purely nonparametric, our approach can be easily implemented to study the property of spherical symmetry of an SPP without a specification of models for the intensity function. Since the computation of the test statistic does not involve estimates of the intensity function, our approach avoids the complicated nonparametric estimation problem.

The article is organized as follows. In Section 2, we propose our test statistic and derive its asymptotic null distribution and power functions. In Section 3, we evaluate the performance of our test statistic by Monte Carlo simulations. We apply our approach to the Japan earthquake data in Section 4. The paper ends with some discussion in Section 5.

2. Methodology

We review the definition of SPPs in Section 2.1, provide the concept of spherical symmetry in Section 2.2, propose our test for the first-order spherical symmetry in Section 2.3, and derive its asymptotic null distribution in Section 2.4. All these subsections are important in the presentation of our approach.

2.1 Spatial Point Processes

An SPP $\mathcal{N}(W)$ in $W \in \mathscr{B}(\mathbb{R}^d)$ is composed of random points in W. It can be treated as the restriction of $\mathcal{N}$, the SPP on the entire $\mathbb{R}^d$, with points only observed in W, implying that points of $\mathcal{N}$ outside of W are unobserved. Let $\mathscr{B}$ and $\mathscr{B}(A)$ be the collections of Borel sets of $\mathbb{R}^d$ and of a measurable $A \subseteq \mathbb{R}^d$, respectively. Then, $N(A)$, the number of points in A, is finite if A is bounded. The SPP $\mathcal{N}$ can be theoretically defined through the Janossy measure approach (Janossy, 1950) or the counting measure approach (Daley and Vere-Jones, 2003). The former is based on distribution functions. The latter is based on intensity functions. Since the two approaches have been shown theoretically equivalent in the literature (Moyal, 1962), and the latter is more popular than the former, we only review the second approach.

The counting measure approach defines the kth-order intensity function of $\mathcal{N}$ as $\lambda_k(\mathbf{s}_1, \ldots, \mathbf{s}_k) = \lim_{\rho(U_{\mathbf{s}_i})\to 0, i=1,\ldots,k} \mathrm{E}\{\prod_{i=1}^k N(U_{\mathbf{s}_i})\}/\prod_{i=1}^k |U_{\mathbf{s}_i}|$, where $\mathbf{s}_1, \ldots, \mathbf{s}_k \in \mathbb{R}^d$ are distinct, $U_{\mathbf{s}}$ is a neighbor of $\mathbf{s}$, $|U_{\mathbf{s}}|$ is its Lebesgue measure, and $\rho(U_{\mathbf{s}})$ is the diameter of $U_{\mathbf{s}}$. The SPP $\mathcal{N}$ is said to be kth-order stationary, if $\lambda_l(\mathbf{s}_1 + \mathbf{h}, \cdots, \mathbf{s}_l + \mathbf{h})$ does not depend on $\mathbf{h}$ for any positive $l \leq k$ with distinct $\mathbf{s}_1, \cdots, \mathbf{s}_l \in \mathbb{R}^d$. It is strong stationary if $\mathcal{N}$ is kth-order stationary for any positive integer k.

The mean structure of $\mathcal{N}$ is

$$\mu(A) = \mathrm{E}\{\mathcal{N}(A)\} = \int_A \lambda(\mathbf{s}) d\mathbf{s}, \tag{1}$$

where $\lambda(\mathbf{s}) = \lambda_1(\mathbf{s})$ is the first-order intensity function. If $\mathcal{N}$ is first-order station-

ary, then $\lambda(\mathbf{s}) = c$ and $\mu(A) = c|A|$, where c is a positive constant. The covariance structure of $\mathcal{N}$ is $\text{cov}\{\mathcal{N}(A_1), \mathcal{N}(A_2)\} = \int_{A_1}\int_{A_2}\{g(\mathbf{s}_1, \mathbf{s_2}) - 1\}\lambda(\mathbf{s}_1)\lambda(\mathbf{s}_2)d\mathbf{s_2}d\mathbf{s_1} + \mu(A_1 \cap A_2)$, where $g(\mathbf{s}_1, \mathbf{s}_2) = \lambda_2(\mathbf{s}_1, \mathbf{s}_2)/\{\lambda(\mathbf{s}_1)\lambda(\mathbf{s}_2)\}$ is the pair correlation function. The variance structure of $\mathcal{N}$ is

$$\text{V}\{\mathcal{N}(A)\} = \int_A \left\{ \int_A [g(\mathbf{s}_1, \mathbf{s}_2) - 1]\lambda(\mathbf{s}_2)d\mathbf{s}_2 + 1 \right\} \lambda(\mathbf{s}_1)d\mathbf{s}_1. \tag{2}$$

If $g(\mathbf{s}_1, \mathbf{s}_2)$ only depends on $\mathbf{s}_1 - \mathbf{s}_2$ or $\|\mathbf{s}_1 - \mathbf{s}_2\|$ such that it can be expressed as $g(\mathbf{s}_1 - \mathbf{s}_2)$ or $g(\|\mathbf{s}_1 - \mathbf{s}_2\|)$, then $\mathcal{N}$ is called a second-order intensity-reweighted stationary or a second-order intensity-reweighted isotropic SPP. This is an important concept for nonstationary SPPs (Baddeley, Møller, and Waagepetersen, 2000).

2.2 Spherical Symmetry

We provide the concept of spherical symmetry for $\mathcal{N}$ on the entire $\mathbb{R}^d$ with $d \geq 2$ based on the counting measure approach. The concept means that intensity functions of $\mathcal{N}$ are invariant under a spherical transformation about a certain point in $\mathbb{R}^d$. It can be extended to a bounded region $W \subseteq \mathbb{R}^d$ if we treat $\mathcal{N}(W)$ as the set of observations.

Assume that $\lambda_k(\mathbf{s}_1, \cdots, \mathbf{s}_k)$ is well-defined for any $k \leq n$. We say $\mathcal{N}$ is nth-order *spherically symmetric* if there exists an $\mathbf{s}_0 \in \mathbb{R}^d$ such that

$$\lambda_k(\mathbf{s}_1, \cdots, \mathbf{s}_k) = \lambda_k(\mathbf{s}_0 + \mathbf{U}(\mathbf{s}_1 - \mathbf{s}_0), \cdots, \mathbf{s}_0 + \mathbf{U}(\mathbf{s}_k - \mathbf{s}_0)), \tag{3}$$

for any $k \leq n$ and any orthogonal matrix $\mathbf{U}$ on $\mathbb{R}^d$. We say that $\mathcal{N}$ is *strongly spherically symmetric* if there exists an $\mathbf{s}_0 \in \mathbb{R}^d$ such that (3) holds for any

$n \in \mathbb{N}$. An SPP $\mathcal{N}(W)$ is nth-order spherically symmetric or strongly spherically symmetric in a measurable $W \subseteq \mathbb{R}^d$ if it can be restricted by an nth-order spherically symmetric or strongly spherically symmetric $\mathcal{N}$ in $\mathbb{R}^d$.

Example 1. *Poisson SPPs. The kth-order intensity function of a Poisson SPP $\mathcal{N}$ is $\lambda_k(\mathbf{s}_1, \cdots, \mathbf{s}_k) = \prod_{i=1}^k \lambda(\mathbf{s}_i)$. If N follows a Poisson distribution with mean κ, then $\lambda(\mathbf{s}) = \kappa f(\mathbf{s})$, implying that $\mathcal{N}$ is strongly spherically symmetric if $f(\mathbf{s})$ is spherically symmetric about some $\mathbf{s}_0$.*

Example 2. *Poisson cluster SPPs. A Poisson cluster SPP $\mathcal{N}$ is derived by first generating parent points from a Poisson SPP with intensity $\varphi(\mathbf{c})$ and then each parent point generating Poisson(η) number of offspring points identically and independently with density $\psi(\mathbf{s}-\mathbf{c})$, where $\mathbf{c}$ and $\mathbf{s}$ represent parent and offspring points, respectively. By Campbell's theorem, we have $\lambda(\mathbf{s}) = \int_{\mathbb{R}^d} \eta\psi(\mathbf{s}-\mathbf{c})\varphi(\mathbf{c})d\mathbf{c}$ and $\lambda_2(\mathbf{s}_1, \mathbf{s}_2) = \int_{\mathbb{R}^d} \eta^2\psi(\mathbf{s}_1-\mathbf{c})\psi(\mathbf{s}_2-\mathbf{c})\varphi(\mathbf{c})d\mathbf{c}+\lambda(\mathbf{s}_1)\lambda(\mathbf{s}_2)$. Thus, $\mathcal{N}$ is strongly spherically symmetric aboud $\mathbf{s}_0$ if ψ is spherically symmetric about $\mathbf{0}$ and φ is spherically symmetric about $\mathbf{s}_0$.*

Example 3. *Second-order intensity-reweighted isotropic (SOIRI) SPPs. The second-order intensity function of an SOIRI SPP $\mathcal{N}$ can be expressed as $\lambda_2(\mathbf{s}_1, \mathbf{s}_2) = [g(\|\mathbf{s}_1 - \mathbf{s}_2\|) - 1]\lambda(\mathbf{s}_1)\lambda(\mathbf{s}_2)$. If $\mathcal{N}$ is first-order spherically symmetric, then there exists an $\mathbf{s}_0 \in \mathbb{R}^d$ such that for any orthogonal matrix $\mathbf{U}$ we have $\lambda_2(\mathbf{s}_0 + \mathbf{U}(\mathbf{s}_1 - \mathbf{s}_0), \mathbf{s}_0 + \mathbf{U}(\mathbf{s}_2 - \mathbf{s}_0)) = [g(\|(\mathbf{s}_0 + \mathbf{U}(\mathbf{s}_1 - \mathbf{s}_0)) - (\mathbf{s}_0 + \mathbf{U}(\mathbf{s}_2 - \mathbf{s}_0))\|) - 1]\lambda(\mathbf{s}_0 + \mathbf{U}(\mathbf{s}_1 - \mathbf{s}_0))\lambda(\mathbf{s}_0 + \mathbf{U}(\mathbf{s}_2 - \mathbf{s}_0)) = [g(\|\mathbf{s}_1 - \mathbf{s}_2\|) - 1]\lambda(\mathbf{s}_1)\lambda(\mathbf{s}_2)$, implying that $\mathcal{N}$ is also second-order spherically symmetric.*

Example 4. *The ETAS (epidemic type aftershock sequence) model. The ETAS model is one of the most important models in the analysis of earthquake clusters. It is defined by a conditional intensity function only affected by ancestors (i.e., mainshocks) but not offsprings (i.e., aftershocks). If an extremely large mainshock earthquake occurs, then within a short time period the ETAS model is primarily dominated by its aftershock patterns. Let the magnitude and the spatiotemporal location of the extremely large mainshock earthquake be denoted by* M^* *and* $(\mathbf{s}^*, t^*)$*, respectively. The conditional intensity function can be approximated by*

$$\lambda^*(\mathbf{s}, t, M) = j(M)\nu(M^*)u(t - t^*)v(\mathbf{s} - \mathbf{s}^*|M^*), \tag{4}$$

where $v(\cdot|M^*)$ *is modeled by a spherically symmetric function at the beginning (Zhuang, Ogata, and Vere-Jones, 2002) and later by an elliptically symmetric function (Ogata and Zhuang, 2006). If a spherically symmetric* $v(\cdot|M^*)$ *is adopted, then the aftershock pattern of earthquake locations can be roughly represented by a spherically symmetric Poisson SPP, indicating that it is strongly spherically symmetric.*

Motivated by the above examples, we find that it is important to justify the first-order spherical symmetry in practice. If an SPP is first-order spherically symmetric, then with a few weak assumptions it may also be second-order spherically symmetric and even strongly spherically symmetric. Therefore, we focus here on proposing a testing method to assess the first-order spherically symmetry.

2.3 A Test for Spherical Symmetry

We propose a Kolmogorov-Smirnov test to assess spherical symmetry. The test is conveniently modified from the classical Kolmogorov-Smirnov test for multivariate distributions. Let $\mathbf{y}$ be a continuous random vector on $\mathbb{R}^p$ with a joint CDF F. If one wants to test a null hypothesis $\mathcal{H}_0 : F = F_0$, then the Kolmogorov-Smirnov statistic for multivariate distributions is given by $K_n = \sup_{\mathbf{y}\in\mathbb{R}^p} \sqrt{n}|\hat{F}(\mathbf{y}) - \hat{F}_0(\mathbf{y})|$, where n is the sample size, $\hat{F}$ is the sample CDF, and $\hat{F}_0$ is the sample CDF under $\mathcal{H}_0$. If data are identically and independently collected, then K_n weakly converges to the absolute value of a certain functional Brownian sheet whose distribution may depend on F_0. Since neither the exact nor the approximate ways are available, a simulation method is often used to compute the p-value of the test.

Without loss of generality, we assume that $\kappa = \int_{\mathbb{R}^d} \lambda(\mathbf{s})d\mathbf{s} < \infty$ and $\mathbf{s}_0 = \mathbf{0}$. We can restrict our method in $\{\mathbf{s} : \|\mathbf{s}\| \leq \eta\}$ for a certain $\eta \in \mathbb{R}^+$ if $\kappa = \infty$. We can make a location shift of coordinates of points if $\mathbf{s}_0 \neq 0$. Then, $\mathcal{N}$ is first-order spherically symmetric if and only if $\lambda(\mathbf{s}) = \lambda_0(r)$, where $\lambda_0(r)$ is the mean of $\lambda(\mathbf{s})$ on the sphere $\{\mathbf{s} : \|\mathbf{s}\| = r\}$. We study a hypothesis testing problem for

$$\mathcal{H}_0 : \lambda(\mathbf{s}) = \lambda_0(\|\mathbf{s}\|), \forall\ \mathbf{s} \in \mathbb{R}^d \tag{5}$$

against

$$\mathcal{H}_1 : \exists\ \mathbf{s} \in \mathbb{R}^d, \text{s.t. } \lambda(\mathbf{s}) \neq \lambda_0(\|\mathbf{s}\|). \tag{6}$$

Let $(z_{\mathbf{s}}, \boldsymbol{\beta}_{\mathbf{s}})$ be the polar coordinates of $\mathbf{s}$, where $z_{\mathbf{s}} \in \mathbb{R}^+$ is the length and $\boldsymbol{\beta}_{\mathbf{s}} =$

$(\beta_1, \cdots, \beta_{(d-1)})^\top \in \Theta = [0, \pi]^{d-2} \times [0, 2\pi]$ is the angle vector of $\mathbf{s}$, respectively. Let $f(\mathbf{s}) = \lambda(\mathbf{s})/\kappa$, $f_0(\mathbf{s}) = \lambda_0(z_\mathbf{s})/\kappa$, $F(r, \boldsymbol{\theta}) = \int_{z_\mathbf{s} \le r, \boldsymbol{\beta}_\mathbf{s} \preceq \boldsymbol{\theta}} f(\mathbf{s}) d\mathbf{s}$, and $F_0(r, \boldsymbol{\theta}) = \int_{z_\mathbf{s} \le r, \boldsymbol{\beta}_\mathbf{s} \preceq \boldsymbol{\theta}} f_0(\mathbf{s}) d\mathbf{s}$ for $r \in \mathbb{R}^+$ and $\boldsymbol{\theta} = (\theta_1, \cdots, \theta_{d-1})^\top \in \Theta$, where $\boldsymbol{\beta} \preceq \boldsymbol{\theta}$ means that $\boldsymbol{\beta}$ precedes $\boldsymbol{\theta}$ which holds if and only if $\beta_j \le \theta_j$ for all $j = 1, \cdots, d$. Then, $f(r, \boldsymbol{\theta})$ and $f_0(r, \boldsymbol{\theta})$ are PDFs (probability density functions) and $F(r, \boldsymbol{\theta})$ and $F_0(r, \boldsymbol{\theta})$ are CDFs (cumulative distribution functions) of r and $\boldsymbol{\theta}$, respectively.

Let $A_r = \{\mathbf{s} : z_\mathbf{s} \le r\}$ and $B_{\boldsymbol{\theta}} = \{\mathbf{s} : \boldsymbol{\beta}_\mathbf{s} \preceq \boldsymbol{\theta}\}$. Then, $A_r \cap B_{\boldsymbol{\theta}} = \{\mathbf{s} : z_\mathbf{s} \le r, \boldsymbol{\beta}_\mathbf{s} \preceq \boldsymbol{\theta}\}$ is a bounded sector region in $\mathbb{R}^d$. For any $\boldsymbol{\theta} \in \Theta$, $F(r, \boldsymbol{\theta})$ and $F_0(r, \boldsymbol{\theta})$ are the expected proportions of points in $A_r \cap B_{\boldsymbol{\theta}}$ under $\mathcal{H}_0 \cup \mathcal{H}_1$ and $\mathcal{H}_0$ given that they are in A_r, respectively. Our Kolmogorov-Smirnov-type statistic is constructed based on the maximum absolute difference between estimators of $F(r, \boldsymbol{\theta})$ and $F_0(r, \boldsymbol{\theta})$.

Let $a_d(\boldsymbol{\theta})$ be the Lebesgue measure of $\{\boldsymbol{\theta}' \in \Theta : \boldsymbol{\theta}' \preceq \boldsymbol{\theta}\}$ proportional to the Lebesgue measure of Θ. Then, $a_d(\boldsymbol{\theta})$ is the CDF of the uniform distribution on Θ. With a few steps of integral calculations, we have $a_d(\boldsymbol{\theta}) = |\Theta|^{-1} \prod_{j=1}^{d-2} c_j(\theta_j)$, where $|\Theta| = 2\pi^{d/2}/\Gamma(d/2)$,

$$c_j(t) = \begin{cases} \text{Beta}(\sin^2 t; \frac{d-j+1}{2}, \frac{1}{2})/2, & 0 \le t \le \pi/2, \\ \text{Beta}(\frac{d-j+1}{2}, \frac{1}{2}) - \text{Beta}(\sin^2 t; \frac{d-j+1}{2}, \frac{1}{2})/2, & \pi/2 < t \le \pi, \end{cases}$$

for $j = 1, \cdots, d-2$, $c_{d-1}(t) = t$ for $t \in [0, 2\pi]$, $\text{Beta}(u, v) = \Gamma(u)\Gamma(v)/\Gamma(u+v)$ is the Beta function, and $\text{Beta}(t; u, v) = \int_0^t z^{u-1}(1-z)^{v-1} dz$ is the incomplete Beta function. We have the following theorem, where the proof of the theorem is given in the online supplementary material.

Theorem 1. *Suppose that $F(r, \boldsymbol{\theta})$ is absolutely continuous with respect to the Lebesgue measure. The necessary and sufficient condition for (5) to be held is that there exists a function $u(r)$ of r such that*

$$F(r, \boldsymbol{\theta}) = a_d(\boldsymbol{\theta})u(r), \tag{7}$$

holds for all $r \in \mathbb{R}^+$ and $\boldsymbol{\theta} \in \Theta$.

Theorem 1 suggests a convenient way for us to propose our test. If we can successfully estimate $F(r, \boldsymbol{\theta})$ and $u(r)$, then we can assess $\mathcal{H}_0$ by testing (7). Since $\mathrm{E}[N(A_r \cap B_{\boldsymbol{\theta}})]/\kappa = F(r, \boldsymbol{\theta})$ and $\mathrm{E}[N(A_r)]/\kappa = u(r)$, $\mathcal{H}_0$ becomes $\mathrm{E}[N(A_r \cap B_{\boldsymbol{\theta}})] = a_d(\boldsymbol{\theta})\mathrm{E}[N(A_r)]$ for all $r \in \mathbb{R}^+$ and $\boldsymbol{\theta} \in \Theta$. Our test statistic has the form

$$T_{d,\xi} = \frac{1}{\xi\sqrt{N}} \sup_{r \in \mathbb{R}^+, \boldsymbol{\theta} \in \Theta} |N(A_r \cap B_{\boldsymbol{\theta}}) - a_d(\boldsymbol{\theta})N(A_r)|, \tag{8}$$

where ξ is an appropriate scaling term to ensure that the test statistic has a standard asymptotic null distribution. Our asymptotic results provide an estimator of ξ^2 as

$$\hat{\xi}^2 = \frac{1}{K-1} \sum_{i=1}^{K} \frac{[N(B_{\Theta_i}) - \hat{N}(B_{\Theta_i})]^2}{\hat{N}(B_{\Theta_i})}, \tag{9}$$

where $B_{\Theta_i} = \{(r, \boldsymbol{\theta}) : \boldsymbol{\theta} \in \Theta_i\}$, $N(B_{\Theta_i})$ is the observed number of points in B_{Θ_i}, $\hat{N}(B_{\Theta_i}) = (|\Theta_i|/|\Theta|)N$ is the estimated number of points in B_{Θ_i}, and $\{\Theta_1, \cdots, \Theta_K\}$ is a partition of Θ. Substituting ξ by $\hat{\xi}$, we get

$$T_d = T_{d,\hat{\xi}} = \frac{1}{\hat{\xi}\sqrt{N}} \sup_{r \in \mathbb{R}^+, \boldsymbol{\theta} \in \Theta} |N(A_r \cap B_{\boldsymbol{\theta}}) - a_d(\boldsymbol{\theta})N(A_r)|. \tag{10}$$

We show in Section 2.4 (i.e., Theorem 3) that the null distribution of T_d can be approximated by the distribution of $\|\mathbb{G}_d\|_\infty = \sup_{(r,\boldsymbol{\theta}) \in [0,1] \times \Theta} |\mathbb{G}_d(r, \boldsymbol{\theta})|$, where

$\mathbb{G}_d$ is a zero mean Gaussian process on $[0,1]\times\Theta$ with a covariance function given by

$$\mathrm{E}\{\mathbb{G}_d[(r,\boldsymbol{\theta})]\mathbb{G}_d[(r',\boldsymbol{\theta}')]\} = (r\wedge r')[a_d(\boldsymbol{\theta}\wedge\boldsymbol{\theta}') - a_d(\boldsymbol{\theta})a_d(\boldsymbol{\theta}')]. \tag{11}$$

We reject $\mathcal{H}_0$ at α significance level if $T_d > \|\mathbb{G}_d\|_{\alpha,\infty}$, where $\|\mathbb{G}_d\|_{\alpha,\infty}$ is the upper α-quantile of the distribution of $\|\mathbb{G}_d\|_\infty$. By a Monte Carlo method, we have $\|\mathbb{G}_2\|_{0.1,\infty} = 1.2937$, $\|\mathbb{G}_2\|_{0.05,\infty} = 1.4250$, and $\|\mathbb{G}_2\|_{0.01,\infty} = 1.6918$. They are used for testing spherical symmetry by T_2. We also have $\|\mathbb{G}_3\|_{0.1,\infty} = 1.5896$, $\|\mathbb{G}_3\|_{0.05,\infty} = 1.7184$, and $\|\mathbb{G}_3\|_{0.01,\infty} = 1.9719$. They are used for testing spherical symmetry by T_3. In particular, we use $\|\mathbb{G}_2\|_{0.05,\infty}$ and $\|\mathbb{G}_2\|_{0.05,\infty}$ in our simulation studies (i.e., Section 3) for the verification of the asymptotic null distributions. We use $\|\mathbb{G}_2\|_{0.05,\infty}$ as well as the simulated distribution of $\|\mathbb{G}_d\|_\infty$ for the significance and the p-value of the test in the analysis of an earthquake data set (i.e., Section 4).

We specify T_d for $d = 2$ and $d = 3$ and numerically evaluate the values of $\|\mathbb{G}\|_{\alpha,\infty}$ by Monte Carlo methods. If $d = 2$, then $a_2(\boldsymbol{\theta}) = \theta/(2\pi)$ where $\boldsymbol{\theta} = \theta \in [0, 2\pi]$, indicating that

$$T_2 = \frac{1}{\hat{\xi}\sqrt{N}} \sup_{r\in\mathbb{R}^+,\theta\in[0,2\pi]} |N(A_r\cap B_\theta) - N(A_r)\theta/(2\pi)|. \tag{12}$$

If $d = 3$, then $a_3(\boldsymbol{\theta}) = (1-\cos\theta_1)\theta_2/(4\pi)$ where $\boldsymbol{\theta} = (\theta_1,\theta_2) \in [0,\pi]\times[0,2\pi]$, indicating that

$$T_3 = \frac{1}{\hat{\xi}\sqrt{N}} \sup_{r\in\mathbb{R}^+,\theta_1\in[0,\pi],\theta_2\in[0,2\pi]} |N(A_r\cap B_{\boldsymbol{\theta}}) - N(A_r)(1-\cos\theta_1)\theta_2/(4\pi)|. \tag{13}$$

Although T_d is presented on the entire space, it can be modified to a bounded

region $W \subseteq \mathbb{R}^d$. If there is an η such that $A_\eta \subseteq W$, then we can restrict $N(A_r \cap B_{\boldsymbol{\theta}})$ and $N(A_r)$ in (10) within A_η, indicating that the superum of T_d is computed under $r \in [0, \eta]$ and $\boldsymbol{\theta} \in \Theta$. In practice, we need to use the largest η satisfying $A_\eta \subseteq W$. We modify observations of the point process by excluding points outside of A_η. To be consistent, we need to modify $\lambda(\mathbf{s})$ by setting $\lambda(\mathbf{s}) = 0$ if $\mathbf{s} \notin A_\eta$. If we define $\kappa = \mathrm{E}[N(A_\eta)]$, then we still have $\kappa < \infty$ and a modified T_d is defined. This problem is to be considered in our simulation studies.

2.4 Asymptotic Distribution

We provide the asymptotic null distribution and power function of T_d under the framework of increasing domain asymptotics with weak dependence. For a bounded observed region W_η of the point pattern, the framework studies the asymptotics under the condition that $|W_\eta| \to \infty$ as $\eta \to \infty$. This approach has been widely adopted in many previous articles. Examples include Guan and Loh (2007), Guan and Shen (2010), Waagepetersen and Guan (2009), Guan, Jalilian, and Waagepetersen (2015), Prekešová and Jensen (2013), and Schoenberg (2005).

The weak dependence is described by the strong mixing condition. Let $\mathscr{B}(E)$ be the collection of Borel sets generated by E. Denote the diameter of E by $\rho(E)$ and the minimum distance between E_1 and E_2 by $\rho(E_1, E_2)$, where $\rho(E) =$

$\sup_{\mathbf{s},\mathbf{s}'\in E}\|\mathbf{s}-\mathbf{s}'\|$ and $\rho(E_1,E_2)=\min_{\mathbf{s}\in E_1,\mathbf{s}'\in E_2}\|\mathbf{s}-\mathbf{s}'\|$. Let

$$\alpha(u,v)=\sup\{|P(U_1\cap U_2)-P(U_1)P(U_2)|:U_1\in\mathscr{B}(E_1),U_2\in\mathscr{B}(E_2),$$
$$\rho(E_1,E_2)\geq u,\rho(E_1)\leq v,\rho(E_2)\leq v,E_1,E_2\in\mathscr{B}(W_\eta)\}$$

be the mixing coefficients, where $P(U)$ is generated by the distribution of $N(U)$. We say that $\mathcal{N}$ is *strongly mixing* if $\alpha(hu,hv)\to 0$ as $h\to\infty$ for any $u,v>0$.

To control the performance of W_η as $\eta\to\infty$, one often assumes that $W_\eta=\eta W=\{\eta\mathbf{s}:\mathbf{s}\in W\}$, where W is a fixed measurable subset of $\mathbb{R}^d$. Without loss of generality, we assume that $W=\{\mathbf{s}:\|\mathbf{s}\|\leq 1\}$ and only points in $W_\eta=\{\mathbf{s}:\|\mathbf{s}\|\leq\eta\}$ are observed. The results of the asymptotics rely on properties of $\phi_\eta(C,D)=\pi(A_C\cap B_D)-a_D\pi_\eta(A_C)$ for $C\subseteq[0,1]$ and $D\subseteq\Theta$, where $A_C=\{\mathbf{s}:z_\mathbf{s}\in C\}$, $B_D=\{\mathbf{s}:\boldsymbol{\beta}_\mathbf{s}\in D\}$, $\pi(E)=\pi_\eta(E)=\mathrm{E}[N_\eta(E)]/\kappa_\eta$ and $N_\eta(E)=N(\eta E)$ for any $E\in\mathscr{B}(W)$, $\kappa_\eta=\mathrm{E}(N_\eta)$, and $N_\eta=N(W_\eta)$. If $\mathcal{H}_0$ holds, then $\phi_\eta(C,D)=0$; otherwise, there exist $C\in\mathscr{B}(W)$ and $D\in\mathscr{B}(\Theta)$ such that $\phi_\eta(C,D)\neq 0$. The primary issue is to show the functional central limit theorem of

$$M_\eta(E)=\eta^{-d/2}\{N_\eta(E)-\mathrm{E}[N_\eta(E)]\},E\subseteq W,$$

under a few scenarios of $\phi_\eta(C,D)$ when $\eta\to\infty$. They provide the asymptotic null distribution, consistency, and local consistency of T_d, respectively. We prove the conclusions by the standard method, which was initially introduced by Ibragimov (1962) and later modified by Herrndorf (1984). The idea is to split any $E\subseteq W$ into two collections of subsets, say $\mathcal{C}$ and $\mathcal{D}$. Both $\mathcal{C}$ and $\mathcal{D}$ can be written into the sum of blocks, where counts in blocks of $\mathcal{C}$ are almost independent and counts in blocks of $\mathcal{D}$ can be ignored. This is a popular idea in the proof

of functional central limit theorem under weak dependence. We only state the theorems here. The proofs of the theorems are given in the online supplementary material.

Theorem 2. *Assume that $\mathcal{N}$ is strongly mixing and there exist positive c_1 and c_2 such that $c_1 \leq \lambda(\mathbf{s}) \leq c_2$ for all $\mathbf{s}$. If the fourth intensity function of $\mathcal{N}$ is uniformly bounded and*

$$\int_0^\infty h^{d-\frac{1}{2}}\alpha(hu, hv)dh < \infty \tag{14}$$

for any positive u and v, then $M_\eta(\cdot)$ weakly converges to a mean zero Gaussian process with independent increments and there exists a measure ν on W such that $\{M_\eta(A_r \cap B_{\boldsymbol{\theta}}) : r \in [0,1], \boldsymbol{\theta} \in \Theta\}$ weakly converges to a d-dimensional mean zero Gaussian process $\mathbb{B}_\nu(\mathbf{t})$ with the covriance function given by

$$\mathrm{E}[\mathbb{B}_\nu(\mathbf{t}_1)\mathbb{B}_\nu(\mathbf{t}_2)] = \nu(A_{r_1 \wedge r_2} \cap B_{\boldsymbol{\theta}_1 \wedge \boldsymbol{\theta}_2}),$$

where $\mathbf{t}_i = (r_i, \theta_{i1}, \cdots, \theta_{i(d-1)}) \in W$ for $i = 1, 2$. If there also exists a constant ω^2 such that

$$\omega^2 = \lim_{\eta \to \infty} \int_{W_\eta} [g(\mathbf{s}, \mathbf{s}') - 1]\lambda(\mathbf{s}')d\mathbf{s}',$$

then $\nu = \xi\mu$, where $\xi = 1 + \omega^2$ and μ is the mean measure generated by the first-order intensity function of $\mathcal{N}$.

Theorem 3. *(Asymptotic null distribution). Suppose that all assumptions of Theorem 2 hold and $\mathcal{H}_0$ also holds. Let $\mathbb{G}_d$ be a mean zero Gaussian process on $[0,1] \times \Theta$ with a covariance function given by (11). Then, $T_d \rightsquigarrow \|\mathbb{G}_d\|_\infty$.*

Theorem 4. *(Consistency). Suppose that there exist* $C \in \mathscr{B}([0,1])$ *and* $D \in \mathscr{B}(\Theta)$ *such that* $|\phi_\eta(C,D)|$ *approaches to a positive number as* $\eta \to \infty$*. For any consistent estimator* $\hat{\xi}^2$ *of* ξ^2*, if all assumptions of Theorem 2 hold but* $\mathcal{H}_0$ *is violated, then* $\lim_{\eta\to\infty} P(T_d \geq c\kappa_\eta^{1/2-\epsilon}) = 1$ *for any positive* ϵ *and* c*.*

Theorem 5. *(Local consistency). Suppose that* $\sup_{r\in[0,1],\boldsymbol{\theta}\in\Theta} |\kappa_\eta^{1/2}\phi_\eta(A_r, B_{\boldsymbol{\theta}})|$ *goes to a bounded constant as* $\eta \to \infty$*. For any consistent estimator* $\hat{\xi}^2$ *of* ξ^2*, if all assumptions of Theorem 2 hold but* $\mathcal{H}_0$ *is violated, then there exists a PDF* $g(\cdot)$ *satisfying* $g(t) > 0$ *for any* $t \in \mathbb{R}^+$ *such that* $\lim_{\eta\to\infty} P(T_d < t) = \int_0^t g(u)du$ *for any* $t \in \mathbb{R}^+$*.*

We provide conclusions about the asymptotic null distribution, the consistency and the local consistency of our test by Theorems 3, 4, and 5, respectively. In particular, Theorem 3 points out that the p-value of test can be approximately calculated by the distribution of $\|\mathbb{G}_d\|_\infty$, where $\mathbb{G}_d$ is a mean zero Gaussian process on $[0,1]\times\Theta$ with the covariance function given by (11). Theorem 4 points out that the power function of the test approaches 1 if $\sup_{C\in\mathscr{B}([0,1]),D\in\mathbb{B}(\Theta)} |\phi_\eta(C,D)|$ does not approach to 0 as $\eta \to \infty$. Note that $\lim_{\eta\to\infty} N_\eta/\kappa_\eta = 1$. Together with Theorem 4, Theorem 5 points out that the optimal rate of the test under the alternative hypothesis is attained.

3. Simulation Studies

We carried out simulation studies to evaluate the performance of our testing method at 0.05 significance level. We simulated realizations from Poisson and

Poisson cluster SPPs in a bounded region $W_\eta = \{\mathbf{s} \in \mathbb{R}^d : \|\mathbf{s}\| \leq \eta\}$ with a varied η. We selected these processes because they are popular in modeling ecological and environmental data. We evaluated type I error probabilities and power functions of T_2 and T_3 as η varied. For a process in $W_\eta \subseteq \mathbb{R}^2$, we chose the first-order intensity function of $\mathcal{N}$ as $\lambda(\mathbf{s}) = \kappa f_\rho(\mathbf{s})$ with $\rho \in [0, 1)$ and $\mathbf{s} = (s_1, s_2) \in W_\eta$, where

$$f_\rho(\mathbf{s}) = f_{2,\rho}(\mathbf{s}) = \frac{1}{2(\eta/3)^2\pi\sqrt{1-\rho^2}} \exp\left\{-\frac{s_1^2 - 2\rho s_1 s_2 + s_2^2}{2(\eta/3)^2\pi(1-\rho^2)}\right\}. \tag{15}$$

In (15), $f_\rho(\mathbf{s})$ was derived by restricting the density of the bivariate normal distribution on W_η with both expected values equal to 0, both variances equal to $(\eta/3)^2$, and the correlation equal to ρ. For a process in $W_\eta \subseteq \mathbb{R}^3$, we chose $\lambda(\mathbf{s}) = \kappa f_\rho(\mathbf{s})$, where $f_\rho(\mathbf{s}) = f_{3,\rho}(\mathbf{s})$ was derived by restricting the density of the three-dimensional normal distribution on W_η with all expected values equal to 0, all variances equal to $(\eta/3)^2$, and all correlations equal to ρ. Therefore, $\lambda(\mathbf{s})$ was spherically symmetric about $\mathbf{0}$ if and only if $\rho = 0$. We set $\kappa = 40\eta^2/9$ which was equivalent to $\eta = (9\kappa/40)^{1/2}$ such that we had a varied κ as η varied.

We followed the standard way to generate Poisson and Poisson cluster SPPs (Guan, 2008, e.g). To obtain a Poisson SPP, we first generated the number of points from the $Poisson(\kappa)$ distribution. We then identically and independently generated the locations of these points from the distribution with density equal to $f_\rho(\mathbf{s})$. To obtain a Poisson cluster SPP, we first generated their parent points from a Poisson SPP with its first-order intensify function equal to $\lambda_p(\mathbf{s}) = \lambda(\mathbf{s})/\gamma$. After that, we generated offspring points based on their corre-

sponding parent points, where each parent point generated $Poisson(\gamma)$ offspring points independently. The position of each offspring point relative to its parent point was defined as a radially symmetric Gaussian random variable with a standard deviation σ. We chose $\gamma = 5$ and $\sigma = 0.02$ in all the cases of Poisson cluster SPPs that we studied. We removed the points which were outside of W_η.

We computed our test statistic for processes on $\mathbb{R}^2$ (i.e., in W_η with $d = 2$) and $\mathbb{R}^3$ (i.e., in W_η with $d = 3$), correspondingly. For a process on $\mathbb{R}^2$, we defined $A_r = \{\mathbf{s} : \|\mathbf{s}\| \leq r\}$ and $B_\theta = \{\beta : 0 \leq \beta \leq \theta\}$, $r \in [0, \eta]$ and $\theta \in [0, 2\pi]$. For an individual $\mathbf{s}_i = (s_{i1}, s_{i2})$, we computed its Euclidean norm value using $\|\mathbf{s}_i\| = (s_{i1}^2 + s_{i2}^2)^{1/2}$ and its angle value using $\beta_i = \arccos(s_{i1}/\|\mathbf{s}_i\|) + \pi I(s_{i2} < 0)$. After that, we calculated $N(A_r \cap B_\theta) = \#\{\mathbf{s}_i : \|\mathbf{s}_i\| \leq r, \beta_i \in [0, \theta]\}$ and $N(A_r) = \#\{\mathbf{s}_i : \|\mathbf{s}_i\| \leq r\}$. We defined our test statistic as

$$T_2 = \frac{1}{\hat{\xi}\sqrt{N}} \sup_{r \in [0,\eta], \theta \in [0,2,\pi]} |N(A_r \cap B_\theta) - N(A_r)\theta/(2\pi)|,$$

where $\hat{\xi}$ was derived by (10) with $K = [N^{1/2}]$ (the greater integer not over $N^{1/2}$) in an equal partitioning way of $[0, 2\pi]$ based on the β_i values. We rejected $\mathcal{H}_0$ if $T_2 > 1.4250$, which was the value of $\|\mathbb{G}_2\|_{0.05,\infty}$ that we have derived via a Monte Carlo method.

For a process on $\mathbb{R}^3$, we defined $A_r = \{\mathbf{s} : \|\mathbf{s}\| \leq r\}$ and $B_{\boldsymbol{\theta}} = \{\boldsymbol{\beta} = (\beta_1, \beta_2) : 0 \leq \beta_1 \leq \theta_1, 0 \leq \beta_2 \leq \theta_2\}$, $r \in [0, \eta]$ and $\boldsymbol{\theta} = (\theta_1, \theta_2) \in [0, \pi] \times [0, 2\pi]$. For an individual $\mathbf{s}_i = (s_{i1}, s_{i2}, s_{i3})$, we computed its Euclidean norm value using $\|\mathbf{s}\| = (s_{i1}^2 + s_{i2}^2 + s_{i3}^2)^{1/2}$ and its angle vectors $\boldsymbol{\beta}_i = (\beta_{i1}, \beta_{i2})$ using $\beta_{i1} = \arccos(s_{i1}/\|\mathbf{s}\|)$ and $\beta_{i2} = \arccos[s_{i2}/(s_{i2}^2 + s_{i3}^2)^{1/2}] + \pi I(s_{i3} < 0)$. After that, we calculated

Table 1: Simulations (with 1,000 replications) for Type I error probabilities ($\rho = 0$) and powers ($\rho > 0$) of T_2 and T_3 for selected κ on W_η with $\eta = (9\kappa/40)^{1/2}$ at 0.05 significance level in Poisson and (Poisson) cluster SPPs, respectively

Test		ρ for Poisson Processes				ρ for Cluster Processes			
Statistic	κ	0.0	0.1	0.2	0.3	0.0	0.1	0.2	0.3
T_2	1,000	0.051	0.099	0.279	0.612	0.046	0.052	0.081	0.148
	2,000	0.045	0.197	0.682	0.976	0.040	0.076	0.145	0.321
	5,000	0.053	0.529	0.999	1.000	0.054	0.102	0.374	0.798
	10,000	0.052	0.898	1.000	1.000	0.053	0.206	0.764	0.997
T_3	1,000	0.053	0.111	0.539	0.933	0.042	0.061	0.076	0.124
	2,000	0.038	0.242	0.950	1.000	0.041	0.070	0.148	0.363
	5,000	0.055	0.774	1.000	1.000	0.053	0.111	0.458	0.889
	10,000	0.048	0.996	1.000	1.000	0.040	0.218	0.878	0.998

$N(A_r \cap B_{\boldsymbol{\theta}})$ and $N(A_r)$ values. We defined our test statistic as

$$T_3 = \frac{1}{\hat{\xi}\sqrt{N}} \sup_{r\in[0,\eta],\theta_1\in[0,\pi],\theta_2[0,2,\pi]} \left|N(A_r \cap B_\theta) - N(A_r)(1-\cos\theta_1)\theta_2/(4\pi)\right|,$$

where $\hat{\xi}$ was also derived by (10) with $K = 2K_0^2$ and $K_0 = [N^{1/3}]$ in an equal partitioning way of $[0,\pi]$ and $[0,2\pi]$ based on the β_{i1} and β_{i2} values, respectively. We rejected $\mathcal{H}_0$ if $T_3 \geq 1.7184$, which was the value of $\|\mathbb{G}_3\|_{0.05,\infty}$ that we have derived via a Monte Carlo method.

We simulated 1,000 realizations for each selected case. We obtained the type I error probabilities and power functions of T_2 and T_3 (Table 1). The results showed that the type I error probabilities (i.e., when $\rho = 0$) were all close

to 0.05, indicating that our asymptotic null distribution provided appropriate ways for the significance of the test. It also indicated that the asymptotic null distribution provided by Theorem 3 was accurate. The power values (i.e., when $\rho > 0$) increased as ρ increased, which was expected as the strength of spherical asymmetry increased with ρ. For the same ρ value, the power increased with κ. This was expected as the expected number of points increased when κ became large. We found that the power values in the Poisson cluster SPPs were lower than those in the Poisson SPPs. The reason was that the performance of the power functions was primarily controlled by the intensity functions of the parent process. As the expected number of parent points was much lower than the value of κ, they were lower than those simulated from the Poisson SPPs.

4. Application

We applied our test to an earthquake data set. Earthquakes are considered as the the most important natural hazard events which often result in numerous deaths and damages. This motivated us to apply our method to earthquake studies. Many sources of earthquake databases have been established and are readily available via Internet. Examples include the websites of the United States National Geophysical (USGS) data center, the Northern California Earthquake Data Center (NCEDC), and many others. These databases contain time and date, depth, locations (given by longitudes and latitudes), and magnitudes at either the regional or the global level from several hundreds years ago to recent

years.

A critical issue in the analysis of earthquake data is to address the impact of earthquake clusters caused by aftershocks. The presence of earthquake clusters often makes it hard to understand the overall patterns of earthquake activities. Many statistical models have been proposed to account for earthquake clusters. Among those, the epidemic-type aftershock sequences (ETAS) model has gained much attention and applied extensively in recent years. The ETAS model is specified by a conditional intensity function. It models the occurrences of offspring (i.e, aftershocks) by clusters triggered by their corresponding ancestors (i.e., mainshocks). Using $(\mathbf{s}_k^*, t_k^*, M_k^*)$ to represent individual mainshock earthquakes, the ETAS model expresses its conditional intensity function for aftershock earthquakes as

$$\lambda(\mathbf{s}, t, M|\mathcal{H}_t) = j(M)[\mu(\mathbf{s}) + \sum_{k:t_k<t} \nu(M_k^*)u(t - t_k^*)v(\mathbf{s} - \mathbf{s}_k^*|M_k^*)],$$

where $j(M)$ is the standardized term, $\mu(\mathbf{s})$ is the background intensity function, $\mathcal{H}_t$ represents the history of mainshock earthquakes occurred before the current time t, and $\nu(M_k^*)$ is the expected number of aftershock from a mainshock ancestor. If an extremely large mainshock earthquake occurs then within a short time period the performance of the ETAS model is primarily dominated by its aftershock earthquakes, implying that the conditional intensity function can be approximately expressed as (4). Since the ETAS model assumes that each mainshock earthquakes produces their aftershock earthquakes independently, aftershock occurrences caused by an extremely large mainshock earthquake can be

roughly treated as a Poisson marked point process (MPP) with the first-order intensity function $\lambda^*(\mathbf{s}, t, M)$ given by (4). If $v(\mathbf{s} - \mathbf{s}^*|M^*) = v(\|\mathbf{s} - \mathbf{s}^*\|M^*)$, then $\lambda^*(\mathbf{s}, t, M)$ is spherically symmetric in the spatial domain. Therefore, we can test spherical symmetry by only considering the spatial locations of the occurrences. Since spatial spherical symmetry is often used as an assumption of the ETAS model, our test is important in the justification of the model. As earthquake hazard maps often fail (Stein, Geller, and Liu, 2012), our test can provide another way to understand earthquake mechanisms.

We collected historical earthquakes from the NCEDC website. We focused on Japan and its neighboring Pacific Ocean regions since Japan is considered the most risky country for earthquakes in the World. We studied earthquake occurrences after January 1, 2000 in these regions and found that most earthquakes occurred in an area between latitude 30 and latitude 45 North, and longitude 130 and 150 East. This area was previously studied for earthquake occurrences (Zhang and Zhuang, 2014; Zhang, 2017). Using this as the study area, we collected earthquake occurrences with magnitudes greater than or equal to 4.0 from January 1, 2000 to December 31, 2016. The data set contained 16,441 earthquakes. There were 1,909 moderate (magnitude ≥ 5 but < 6), 201 strong (magnitude ≥ 6 but < 7), 20 major (magnitude ≥ 7 but < 8), and 2 great (magnitude ≥ 8) earthquakes. The most serious one was the *Great Tohoku Earthquake* occurred in March 11, 2011 at 38.30 latitude North and 142.37 longitude East with magnitude 9.1. It caused about sixteen thousand people deaths and a seri-

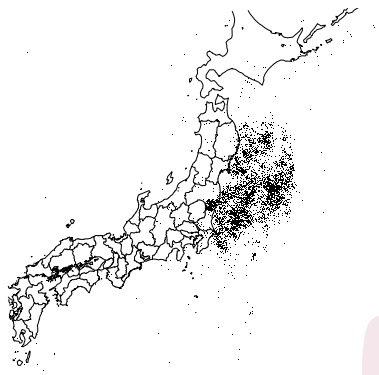

Figure 1: Aftershock earthquakes within the first 180 days of the *2011 Great Tohoku Earthquake*.

ous nuclear accident in Fukushima Nuclear Power Plants, affecting hundreds of thousands of residents in a few thousand square kilometers area.

Since the magnitude of *2011 Great Tohoku Earthquake* was extremely large, we can approximately use (4) to model its aftershock pattern. Note that M^*, t^* and $\mathbf{s}^*$ are only related to the information of the mainshock earthquake. They can be treated as known constants in (4), indicating that the spatial margin of $\lambda^*(\mathbf{s}, t, M)$ becomes

$$\lambda(\mathbf{s}) = \kappa v(\mathbf{s} - \mathbf{s}^* | M^*), \tag{16}$$

where $\kappa = \nu(M^*) \int_0^\infty j(M) dM \int_0^\infty u(t - t^*) dt$. Thus, $\lambda^*(\mathbf{s}, t, M)$ is spherical symmetric if and only if $\lambda(\mathbf{s})$ is spherical symmetric about $\mathbf{s}^*$, indicating that we can take $\mathbf{s}_0 = \mathbf{s}^*$ in our test.

We focused on earthquake aftershock activities within the first 180 days after the occurrence of the *Great Tohoku Earthquake*. The data set contained

4,503 earthquakes with magnitudes greater than or equal to 4.0, which included 0 great, 4 major, 73 strong, and 652 moderate earthquakes. We used T_2 to test spherical symmetry of $\lambda(\mathbf{s})$ given by (16). To derive the value of T_2, we computed the spherical distance between the locations of aftershock and the mainshock earthquakes and the angles between the direction of aftershock earthquakes to the mainshock earthquakes and the direction of the east. We also computed the value of $\hat{\xi}^2$ using the same way as we did in our simulation studies. We calculated the p-value of T_2 based on the simulated distribution of $\|\mathbb{G}_2\|_\infty$. We rejected $\mathcal{H}_0$ and concluded significance of the test if $T_2 > 1.4250$ as the upper 0.05 quantile of the simulated distribution of $\|\mathbb{G}_2\|_\infty$ was 1.4250. We tested spherical symmetry for aftershock earthquakes within a few options of periods starting from the occurrence of the *Great Tohoku Earthquake* (Table 2). We concluded that the spherical symmetry was generally correct at the beginning, but slightly violated at the end of the period. Based on our results, we concluded that the ETAS model was able to account for the aftershock earthquake clusters in the Japan and its neighboring areas.

5. Discussion

In this article, we provide a Kolmogorov-Smirnov-type test to assess first-order spherical symmetry of SPPs. The test is modified from the classical Kolmogorov-Smirnov test for multivariate distributions. The classical test is formulated under the assumption that sampling data are independently and independently

Table 2: Test for spherical symmetry of aftershock earthquakes within the first m days starting from the occurrence of the *Great Tohoku Earthquake*.

	Number of Aftershock Earthquakes					
m	Total	Major	Strong	Moderate	T_2	p-value
1	671	2	42	261	1.1088	0.2218
2	1,108	2	45	324	1.2688	0.1066
3	1,410	2	45	361	1.3684	0.0663
10	2,238	2	48	459	1.6928	0.0102
30	3,047	3	56	528	1.9090	0.0030
180	4,503	4	73	652	2.1782	0.0003

collected. This assumption is violated because of the existence of dependence in spatial point data. We propose a way to account for the dependence via a dispersion parameter. Using our asymptotic theory, we present a method to approximately interpret the dispersion parameter by the well-known quasi-Poisson model in the statistical literature, which provides an estimator of the parameter. Our test statistic is derived after the classical statistic is adjusted by the estimator of the dispersion parameter. As our test statistic does not involve nonparametric smoothning techniques, our test can be consistent with the optimal rate (i.e. Theorems 4 and 5). Therefore, our test is asymptotically more powerful than any other test involving nonparametric smoothing techniques. Our method can also be modified to the Cramér-von Mises-type approach.

An obvious advantage is that the asymptotic null distribution of our test

statistic does not rely on the unknown underlying intensity function. It has been acknowledged for a long time that the asymptotic null distribution of an empirical statistic for multivariate distributions, such as the Kolmogorov-Smirnov or the Cramér-von Mises statistics, depends on the underlying distribution, making the computation of their asymptotical p-values complicated (Zhang and Zhuang, 2017). The asymptotic null distribution of a goodness-of-fit statistic in the one-dimenional case is often related to the distribution of a norm of the standard Brownian bridge, which may have a closed form expression (van der Vaart, 1998, P. 297). The nice property makes it easy to implement goodness-of-fit tests for univariate distributions. Although the concept of the standard Brownian bridge has been extended to its high-dimensional version called Brownian sheets, it is still hard to implement goodness-of-fit tests for multivariate random variables because neither the exact nor the approximate null distribution is available. Our research provides a way to implement this approach.

Testing nice properties of intensity functions of SPPs is important in practice. The problem studied in this article is only related to first-order spherical symmetry. It does not contain any specification of second-order properties. Therefore, the selection of statistical models for the second-order properties is flexible. Because of the popularity of the SOIRS, one can also model the second-order intensity function under first-order spherical symmetry together, which provides a way to jointly analyze the first-order and second-order intensity functions. This is an important research question in the future.

Supplementary Materials

The online supplememntary material includes the proofs of Theorems 1, 2, 3, 4, and 5 as well as their associated lemmas.

Acknowledgement: The authors appreciates comments from an associate editor and two anonymous referees, that significantly improve the quality of the article.

References

Baddeley, A.J., Møller, J. and Waagepetersen, R. (2000). Non- and semi-parametric estimation of interaction in inhomogeneous point patterns. *Statistica Neerlandica*, **54**, 329-350.

Balderama, E., Schoenberg, F.P., Murray, E., and Rundel, P.W. (2012). Application of branching models in the study of invasive species. *Journal of the American Statistical Association*, **107**, 467-476.

Besag, J. (1977). Contribution to the discussion of Dr. Ripley's paper. *Journal of the Royal Statistical Society Series B*, **39**, 193-195.

Brandwein, A.C., and Strawderman, W.E. (1991). Generalizations of James-Stein estimators under spherical symmetry. *Annals of Statistics*, **19**, 1639-1650.

Daley, D.J. and Vere-Jones, D. (2003). *An Introduction to Theory of Point Processes: Volume I: Elementary Theory and Methods, Second Edition.* Springer, New York.

Diggle, P.J. (1985). A kernel method for smoothing point process data. *Applied Statistics*, **34**, 138-147.

Diggle, P.J. (2003). *Statistical Analysis of Spatial Point Patterns, 2nd Edition*, New York: Wiley.

Diggle, P.J. (2006). Spatio-temporal point processes, partial likelihood, foot and mouth disease. *Statistical Methods in Medical Research*, **16**, 325-336.

Guan, Y. abd Loh, J.M. (2007). A thinned block bootstrap variance estimation procedure for inhomogeneous spatial point patterns. *Journal of the American Statistical Association*, **102**, 1377-1386.

Guan, Y. (2008). A KPSS test for stationarity for spatial point processes. *Biometrics*, **64**, 800-806.

Guan, Y. and Shen, Y. (2010). A weighted estimating equation approach for inhomogeneous spatial point processes. *Biometrika*, **97**, 867-880.

Guan, Y., Jalilian, A., Waagepetersen, R. (2015). Quasi-likelihood for spatial point processes. *Journal of Ryal Statistial Society Series B*, **77**, 677-697.

Hall, P., Watson, G.S., and Cabrera, J. (1987). Kernel density estimation with spherical data. *Biometrika*, **74**, 751-762.

Henrys, P.A. and Brown, P.E. (2009). Inference for cluster inhomogeneous spatial point processes. *Biometrics*, **65**, 423-430.

Henze, N., Hlávka, Z., and Meintanis, S.G. (2014). Testing for spherical symmetry via the empirical characetristic function. *Statistics*, **48**, 1282-1296.

Herrndorf, N. (1984). A functional central limit theorem for weakly dependent sequence of random variables. *Annals of Probability*, **12**, 141-153.

Ibragimov, I.A. (1962). Some limit theorems for stationary processes. *Stochastic Processes and Their Applications*, **12**, 171-186.

Janossy, L. (1950). On the absorption of a nucleon cascade. *Proceedings of the Royal Irish Academy A*, **53**, 181-888.

Justel A, Peña D, Zamar R. (1997). A multivariate Kolmogorov-Smirnov test of goodness of fit. *Statistics and Probability Letters*, **35**, 251-259.

Meyer, S. and Held, L. (2014). Power-law models for infectious disease spread. *Annals of Applied Statistics*, **8**, 1612-1639.

Møller, J. and Waagepetersen, R.P. (2007). Modern statistics for spatial point processes (with discussion). *Scandinavian Journal of Statistics*, **34**, 685-711.

Moyal, J.E. (1962). The general theory of Stochastic population processes. *Acta Mathematics*, **108**, 1-31.

Myllymäki, M. and Penttinen, A. (2009). Conditionally heteroscedastic intensity-dependent marking of log Gaussian Cox processes. *Statistica Neerlandica*, **63**, 450-473.

Ogata, Y. (1988). Statistical models for earthquake occurrences and residual analysis for point processes. *Journal of the American Statistical Association*, **83**, 9-27.

Ogata, Y. and Zhuang, J. (2006). Space-time ETAS models and an improved extension. *Techonophysics*, **413**, 13-24.

Peng, R.D., Schoenberg, F.P, and Woods, J.A. (2005). A space-time conditional intensity model for evaluating a wildfire hazard index. *Journal of the American Statistical Association*, **100**, 26-35.

Prekešová, M. and Jensen, V.B.V. (2013). Asymptotic palm likelihood theory for stationary point processes. *Annals of Institute of Statistical Mathematics*, **65**, 387-412.

Ripley, B.D. (1976). The second-order analysis of spatial point processes. *Journal of Applied Probability*, **23**, 255-266.

Schoenberg, F.P. (2005). Consistent parametric estimation of the intensity of a spatial-temporal point process. *Journal of Statistical Planning and Inference*, **128**, 79-93.

Stein, S., Geller, R.J., and Liu, M. (2012). Why earthquake hazard maps often fail and what to do about it. *Tectonophysics*, **562-563**, 046102.

Stoyan, D. and Stoyan, H. (1994). *Fractals, Random Shapes and Point Fields.* New York: Wiley.

Stoyan, D. and Stoyan, H. (1996). Estimating pair correlation functions of planar cluster processes. *Biometrical Journal*, **38**, 259-271.

van der Vaart, A.W. (1998). *Asymptotic Statistics*, Cambridge University Press, Cambridge, UK.

Waagepetersen, R. (2007). An estimating function approach to inference for inhomogeneous Neyman-Scott process. *Biometrics*, **63**, 252-258.

Waagepetersen, R. and Guan, Y. (2009). Two-step estimation for inhomogeneous spatial point processes. *Journal of the Royal Statistical Society B*, **71**, 685-702.

Zhang, T. and Zhuang, Q. (2014). On the local odds ratio between points and marks in marked point processes. *Spatial Statistics*, **9**, 20-37.

Zhang, T. and Zhou, B. (2014). Test for stationarity for spatial point processes in an arbitrary region. *Journal of Agricultural, Biological and Environmental Statistics*, **19**, 387-404.

Zhang, T. (2014). A Kolmogorov-Smirnov type test for independence between marks and points of marked point processes. *Electronic Journal of Statistics*, **8**, 2557-2584.

Zhang, T. and Zhuang, R. (2017). Testing proportionality between the first-order intensity functions of spatial point processes. *Journal of Multivariate Analysis*, **155**, 72-82.

Zhang, T. (2017). On independence and separability between points and marks of marked point processes. *Statistica Sinica*, **27**, 207-227.

Zhuang, J., Ogata, Y., and Vere-Jones, D. (2002). Stochastic declustering of spacetime earthquake occurrences. *Journal of the American Statistical Association*, **97**, 369-380.